International Journal of Nanomedicine

Dovepress
open access to scientific and medical research

Open Access Full Text Article

ORIGINAL RESEARCH

Optical imaging of absorption and distribution of RITC-SiO_2 nanoparticles after oral administration

This article was published in the following Dove Press journal:
International Journal of Nanomedicine
15 December 2014
Number of times this article has been viewed

Chang-Moon Lee[1]
Tai Kyoung Lee[2–5]
Dae-Ik Kim[1,6]
Yu-Ri Kim[7]
Meyoung-Kon Kim[7]
Hwan-Jeong Jeong[2–5]
Myung-Hee Sohn[2–5]
Seok Tae Lim[2–5]

[1]Department of Biomedical Engineering, Chonnam National University, Yeosu, Jeollanam-Do, Republic of Korea; [2]Department of Nuclear Medicine, Chonbuk National University Medical School and Hospital, Jeonju, Jeollabuk-Do, Republic of Korea; [3]Cyclotron Research Center, Chonbuk National University Medical School and Hospital, Jeonju, Jeollabuk-Do, Republic of Korea; [4]Biomedical Research Institute, Chonbuk National University Medical School and Hospital, Jeonju, Jeollabuk-Do, Republic of Korea; [5]Molecular Imaging and Therapeutic Medicine Research Center, Chonbuk National University Medical School and Hospital, Jeonju, Jeollabuk-Do, Republic of Korea; [6]School of Electrical, Electronic Communication, and Computer Engineering, Chonnam National University, Yeosu, Jeollanam-Do, Republic of Korea; [7]Department of Biochemistry and Molecular Biology, Korea University Medical School and College, Seounbuk-Gu, Seoul, Republic of Korea

Correspondence: Seok Tae Lim
Department of Nuclear Medicine, Chonbuk National University Medical School and Hospital, 634-18, Geumam-2 dong, Dukjin-gu, Jeonju, Jeonbuk 561-712, Republic of Korea
Tel +82 63 250 1172
Fax +82 63 255 1172
Email stlim@chonbuk.ac.kr

Purpose: In this study, we investigated the absorption and distribution of rhodamine B isothiocyanate (RITC)-incorporated silica oxide nanoparticles(SiNPs) (RITC-SiNPs) after oral exposure, by conducting optical imaging, with a focus on tracking the movement of RITC-SiNPs of different particle size and surface charge.

Methods: RITC-SiNPs (20 or 100 nm; positively or negatively charged) were used to avoid the dissociation of a fluorescent dye from nanoparticles via spontaneous or enzyme-catalyzed reactions in vivo. The changes in the nanoparticle sizes and shapes were investigated in an HCl solution for 6 hours. RITC-SiNPs were orally administered to healthy nude mice at a dose of 100 mg/kg. Optical imaging studies were performed at 2, 4, and 6 hours after oral administration. The mice were sacrificed at 2, 4, 6, and 10 hours post-administration, and ex vivo imaging studies were performed.

Results: The RITC-SiNPs were stable in the HCl solution for 6 hours, without dissociation of RITC from the nanoparticles and without changes in size and shape. RITC-SiNPs flowed into the small intestine from the stomach and gradually moved along the gut during the experiment. In the ex vivo imaging studies, optical signals were observed mostly in the lungs, liver, pancreas, and kidneys. The orally administered RITC-SiNPs, which were absorbed in the systemic circulation, were eliminated from the body into the urine. The 20 nm RITC-SiNPs showed higher uptake in the lungs than the 100 nm RITC-SiNPs. The distribution of the 100 nm RITC-SiNPs in the liver was higher than that of the 20 nm RITC-SiNPs, but the differences in the surface charge behavior were imperceptible.

Conclusion: We demonstrated that the movement of RITC-SiNPs after oral exposure could be traced by optical imaging. Optical imaging has the potential to provide valuable information that will help in understanding the behavior of SiNPs in the body following exposure.

Keywords: silica nanoparticles, oral exposure, rhodamine B isothiocyanate, RITC-SiNP

Introduction

Silica-based nanoparticles (SiNPs) have attracted increasing interest in various biomedical and industrial fields because they can be prepared by a simple synthetic process and with unique properties, such as easy surface modification, tunable particle size, and specific surface area.[1–3] As the use of SiNPs increased and spread to various other applications, the interests in SiNPs shifted from their applications towards their safety for humans.[4] Recently, Gong et al[5] reported that exposure to SiNPs results in a concentration- and size-dependent cytotoxicity and DNA (deoxyribonucleic acid) damage in cultural HaCaT (keratinocyte) cells. Therefore, it would be very important to understand the process of absorption and distribution of SiNPs upon entering the body through the respiratory system or the skin. In addition, it would be essential to

determine the changes in biodistribution, according to the differences in the properties of nanomaterials, since the fate of nanomaterials in the body would be dependent on their physicochemical characteristics such as particle size, morphology, and surface properties.[6]

The behavior of nanomaterials entering the body can be tracked by tagging an optical dye onto the nanomaterials, labeling nanomaterials with a radioisotope, or direct radiolabeling.[7–9] Traceable nanomaterials can provide good noninvasive approaches to answer important questions in understanding their pharmacokinetic behaviors in vivo. However, the chemical conjugation of an optical dye and a radioisotope to the nanomaterials can be susceptible to the dissociation in the in vivo environments if the dye and radioisotope are not protected from the media.[10,11] In addition, surface modification of the nanomaterials to attach a tracer may change their behavior in the body and alter their absorption and biodistribution, because the surface properties of the nanomaterials could undergo unwanted alterations as a result of surface engineering.[12]

Recently, cyclotron-based irradiation techniques have been used for directly radiolabeling nanomaterials and for investigating their biodistribution and nanotoxicology.[9] For example, Chen et al[13] used radioactive ^{69m}ZnO nanoparticles to determine their tissue concentrations by tracking them after intravenous administration in mice. The radioactive nanoparticles revealed the advantages of convenient preparation, since surface modification would not be required with tagging imaging probes onto the nanomaterials, allowing minimal changes in their surface properties and preventing any alteration of their distribution or fate in vivo. Ultimately, the use of radioactive nanoparticles would be a better approach for tracing the nanomaterials in vivo without the need for transformative surface modification. In the case of SiNPs, a fluorescent dye was incorporated, and shielded colloidal particles inside during the preparation procedure.

In this present study, the distribution and fate of rhodamine B isothiocyanate (RITC)-incorporated SiNPs (RITC-SiNPs) were studied for better understanding of their safety in vivo by following oral exposure with an optical imaging system. To examine the influence of particle size and surface charge on the fate and distribution of RITC-SiNPs after their oral administration, four different types of RITC-SiNPs, 20 nm positively charged RITC-SiNPs, 20 nm negatively charged RITC-SiNPs, 100 nm positively charged RITC-SiNPs, and 100 nm negatively charged RITC-SiNPs were investigated.

Materials and methods

Materials and animals

Four types of RITC-SiNPs (RITC-SiNPs$^{20(+)}$, 20 nm positively charged; RITC-SiNPs$^{20(-)}$, 20 nm negatively charged; RITC-SiNPs$^{100(+)}$, 100 nm positively charged; and RITC-SiNPs$^{100(-)}$, 100 nm negatively charged) were obtained from IMGT Co, Ltd, (Suwon, Republic of Korea). Female athymic nude mice (5 weeks old and weighing 18–20 g) were purchased from Orient Bio Inc., (Seongnam, Republic of Korea).

Characterization and stability of RITC-SiNPs

The four types of RITC-SiNPs were examined by transmission electron microscopy (TEM), and their surface charge was characterized by using a zeta potential and particle size analyzer (ELS-8000; Photal Otsuka Electronics Co, Ltd, Osaka, Japan). The RITC-incorporated SiNPs (1 mg) were suspended in 5 mL saline and HCl solution (0.7% v/v, pH 1.2) at 37°C for 7 hours. The dissociation of RITC from the SiNPs was determined by detecting the absorbance of RITC with an ultraviolet spectrophotometer at every scheduled time point. At 7 hours after the dissociation test, the SiNPs were observed by TEM to evaluate their morphological changes in the HCl solution.

In vivo optical imaging study

All animal experiments were performed in accordance with guidelines suggested by the Chonbuk National University Medical School Committee. The four types of RITC-SiNPs (2 mg/0.2 mL distilled water) were administered orally into the healthy nude mice using a sonde. All optical imaging experiments were performed with an IVIS® (Caliper LifeSciences, Hopkinton, MA, USA) spectrum small-animal in vivo imaging system. After oral administration to the nude mice, whole-body optical images were obtained at 2, 4, and 6 hours (n=4). The following settings were used: excitation wavelength (540 nm), emission wavelength (580 nm), exposure time (3 seconds), f/stop (2), binning (8), and field of view (12.8 cm). After acquiring in vivo optical images, the background images were subtracted from the images of the mice using Living Image (Caliper LifeSciences) software. To remove tissue autofluorescence from image data, the IVIS Imaging System (Caliper LifeSciences) implements a substraction method using blue-shifted background filters that emit light at a shorter wavelength (460–490 nm).

Ex vivo optical imaging study

After the in vivo optical imaging study, we performed the ex vivo optical imaging study to investigate the absorption

of RITC-SiNPs from the gastrointestinal (GI) tract into the body and their distributions in various organs. The mice were sacrificed after in vivo optical imaging at 2, 4, 6, and 10 hours (n=4). The major organs, such as the brain, heart, lungs, liver, spleen, pancreas, kidneys, muscle, and bone, were collected and imaged ex vivo. The acquired images were analyzed by IVIS Living Image software.

Results

All RITC-SiNPs had a uniform spherical shape (Figure 1). The zeta potential values of RITC-SiNPs$^{20(+)}$, RITC-SiNPs$^{20(-)}$, RITC-SiNPs$^{100(+)}$, and RITC-SiNPs$^{100(-)}$ were 37.3, −13.4, 32.5, and −43.5 mV, respectively (Figure 2). All RITC-SiNPs showed excitation wavelength (λ_{ex}) of 543 nm and emission wavelength (λ_{em}) of 580 nm. As shown in Figure 3, all RITC-SiNPs had a similar shape and particle size after incubation in the HCl solution at 37°C. A small amount (2%–4% of the total RITC fluorescence activity) of RITC was released from the 20 nm RITC-SiNPs during incubation in the HCl solution (pH 1.2), whereas release and dissociation of free RITC from the 100 nm RITC-SiNPs and the degradation of RITC were not observed (Figure 4).

Figure 5 shows the whole-body optical fluorescence images of mice after oral administration of the RITC-SiNPs. The fluorescence signals from the RITC-SiNPs were mainly visualized in the GI tract of the mice after oral administration of the RITC-SiNPs. Ex vivo optical images of the major organs from the mice are presented in Figure 6. Quantification results of ex vivo images were shown in Figure 7. After their oral administration of the RITC-SiNPs, majority of them was found to be distributed in the lungs, liver, pancreas, and kidneys. The RITC-SiNPs with a diameter of 20 nm showed higher uptake in the lungs than the RITC-SiNPs with a diameter of 100 nm. After their oral administration, no differences in the translocation and distribution of RITC-SiNPs were observed because of their surface charges. At 10 hours post-administration, the majority of 20 nm RITC-SiNPs were cleared from the organs, and they were visualized in the kidneys. On the other hand, the 100 nm RITC-SiNPs were distributed mainly in the liver and kidneys, and they were cleared from the organs except for the kidneys at 10 hours after oral administration.

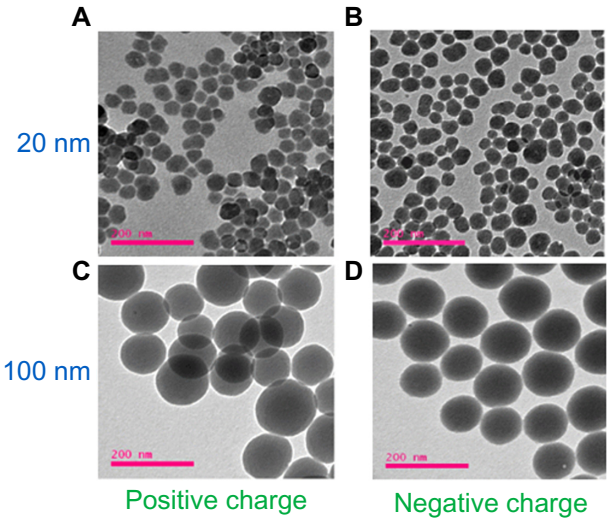

Figure 1 Transmission electron microscopy images of RITC-SiNPs: (**A**) RITC-SiNPs$^{20(+)}$, (**B**) RITC-SiNPs$^{20(-)}$, (**C**) RITC-SiNPs$^{100(+)}$, and (**D**) RITC-SiNPs$^{100(-)}$.
Note: Scale bar =200 nm.
Abbreviations: RITC-SiNP, rhodamine B isothiocyanate-incorporated silica oxide nanoparticle; RITC-SiNPs$^{20(+)}$, 20 nm positively charged RITC-SiNPs; RITC-SiNPs$^{20(-)}$, 20 nm negatively charged RITC-SiNPs; RITC-SiNPs$^{100(+)}$, 100 nm positively charged RITC-SiNPs; RITC-SiNPs$^{100(-)}$, 100 nm negatively charged RITC-SiNPs.

Discussion

As a result of the rapid growth of nanotechnology, it has become essential to understand the toxicity and kinetics of nanomaterials upon exposure into the body through dermal, oral, or respiratory routes. Recently, Yu et al[1] reported that amorphous SiNPs of a diameter of 64.4 nm induces injuries to the liver, spleen, and lungs after intravenous administration to ICR (imprinting control region) mice. In previous papers, atomic absorption spectrometry has been widely used to determine the accumulated nanomaterials in the organs through elemental analysis of nanomaterials. In this present study, the main aim was to evaluate distribution of SiNPs through optical imaging and use RITC-SiNPs. To trace the movement and to monitor the kinetics of nanomaterials upon administration into the body, chemical surface modification by attaching a tracer to the nanomaterials became necessary. However, surface modification can lead to changes in surface properties and particle size. Because the absorption of orally administered nanomaterials into the body depends greatly on their size and surface charge, it is be better to use nanomaterials without surface modification by attaching a tracer.[14,15] The dissociation and breakage of the tracer from nanomaterials should also be assessed in the biological fluid. RITC-SiNPs were prepared with the RITC-aminopropyltriethoxysilane (APTS) conjugate according to a previously described method.[16] The positively charged SiNPs were designed using an excess free APTS, whereas the negatively charged SiNPs were prepared without free APTS. Thus, the positively charged and negatively charged SiNPs have many amino groups and hydroxyl groups on their surface, respectively.

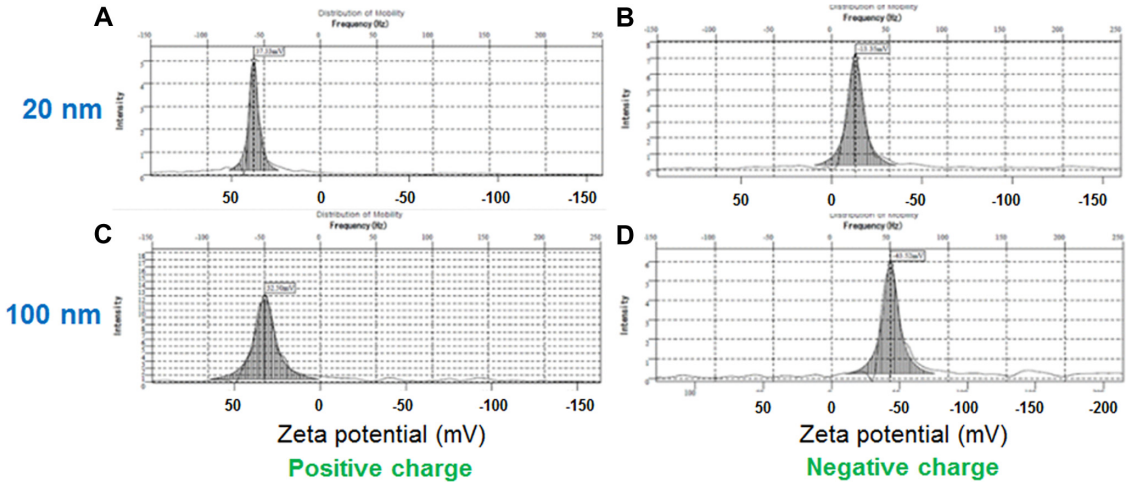

Figure 2 Zeta potential spectra of RITC-SiNPs: (**A**) RITC-SiNPs$^{20(+)}$, (**B**) RITC-SiNPs$^{20(-)}$, (**C**) RITC-SiNPs$^{100(+)}$, and (**D**) RITC-SiNPs$^{100(-)}$.
Abbreviations: RITC-SiNP, rhodamine B isothiocyanate-incorporated silica oxide nanoparticle; RITC-SiNPs$^{20(+)}$, 20 nm positively charged RITC-SiNPs; RITC-SiNPs$^{20(-)}$, 20 nm negatively charged RITC-SiNPs; RITC-SiNPs$^{100(+)}$, 100 nm positively charged RITC-SiNPs; RITC-SiNPs$^{100(-)}$, 100 nm negatively charged RITC-SiNPs.

In this present study, the absorptions and distributions of RITC-SiNPs were investigated after their oral administration, without surface modification. RITC, a fluorescent dye for tracing the orally administered SiNPs in vivo, was incorporated into the nanoparticles without surface modification and conjugation. To examine the effects of different particle sizes and surface charges on the absorption and distribution of RITC-SiNPs after oral exposure, negatively and positively charged RITC-SiNPs of different sizes (20 and 100 nm) were used.

The distributions, clearances, and biocompatibility of absorbed SiNPs in the systemic circulation were primarily dependent on particle shape.[17] As shown in Figure 1, all RITC-SiNPs used in this study had a spherical shape with an aspect ratio of ~1. Although the distributions and clearances of conjugated nanoparticles with a radioisotope or a fluorescent dye in the body can be traced by using imaging techniques, it is very important to assess the dissociation of a radioisotope or a fluorescent dye from the nanoparticles by spontaneous or enzyme-catalyzed reactions in vivo. After immersing and incubating the RITC-SiNPs into the HCl solution (pH 1.2) or distilled water for 6 hours at 37°C, TEM analyses of the RITC-SiNPs did not show any change in their shape (Figure 3). The dissociation of RITC from the RITC-SiNPs was investigated under similar conditions (pH 1.2) in the stomach (Figure 4). The release of RITC from the 100 nm RITC-SiNPs was not detected, whereas minimal dissociation of RITC from the 20 nm RITC-SiNPs was observed.

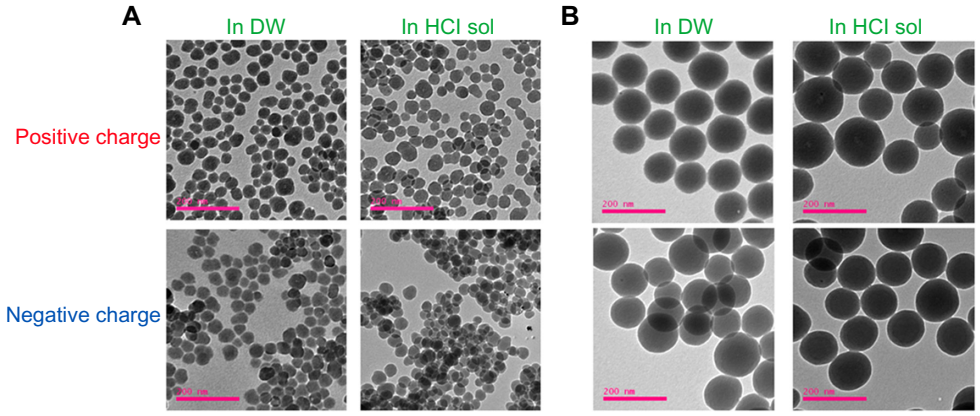

Figure 3 TEM images of (**A**) RITC-SiNPs$^{20(+)}$ and RITC-SiNPs$^{20(-)}$, (**B**) RITC-SiNPs$^{100(+)}$, and RITC-SiNPs$^{100(-)}$ for determining their in vitro stability in distilled water and HCl solution (pH 1.2). The TEM images of RITC-SiNPs were obtained at 6 hours after immersion in distilled water and HCl solution (pH 1.2) at 37°C.
Note: Scale bar =200 nm.
Abbreviations: DW, distilled water; RITC-SiNP, rhodamine B isothiocyanate-incorporated silica oxide nanoparticle; RITC-SiNPs$^{20(+)}$, 20 nm positively charged RITC-SiNPs; RITC-SiNPs$^{20(-)}$, 20 nm negatively charged RITC-SiNPs; RITC-SiNPs$^{100(+)}$, 100 nm positively charged RITC-SiNPs; RITC-SiNPs$^{100(-)}$, 100 nm negatively charged RITC-SiNPs; TEM, transmission electron microscopy; sol, solution.

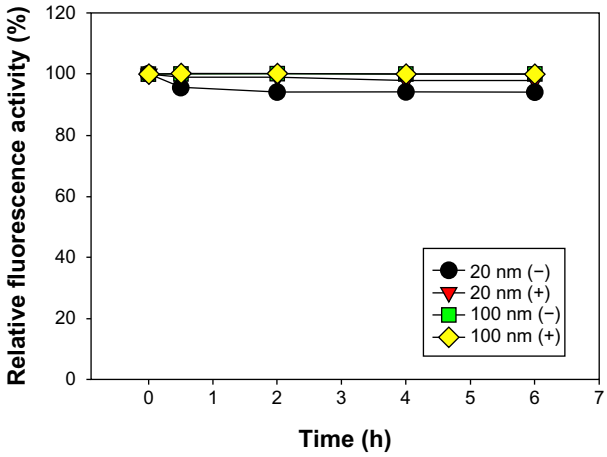

Figure 4 An in vitro stability study of RITC-SiNPs for 6 hours (h) after immersion in the HCl solution (pH 1.2) at 37°C. The dissociation and release of RITC from RITC-SiNPs were detected using an ultraviolet spectrophotometer and expressed as the relative fluorescence activity of RITC-SiNPs in comparison with their initial fluorescence activity.
Abbreviations: RITC, rhodamine B isothiocyanate; RITC-SiNP, RITC-incorporated silica oxide nanoparticle.

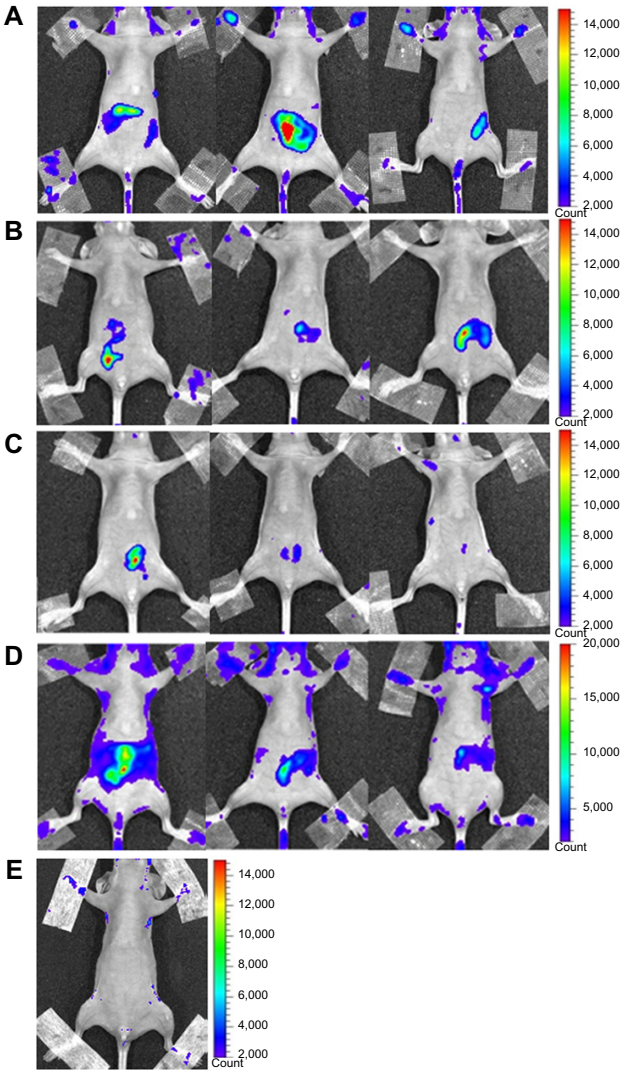

Figure 5 In vivo optical images of mice that were orally administered with: (**A**) RITC-SiNPs$^{20(+)}$, (**B**) RITC-SiNPs$^{20(-)}$, (**C**) RITC-SiNPs$^{100(+)}$, and (**D**) RITC-SiNPs$^{100(-)}$ at 2, 4, and 6 hours post-administration. (**E**) A healthy mouse without administration of RITC-SiNPs and imaged under the same conditions.
Abbreviations: RITC-SiNP, rhodamine B isothiocyanate-incorporated silica oxide nanoparticle; RITC-SiNPs$^{20(+)}$, 20 nm positively charged RITC-SiNPs; RITC-SiNPs$^{20(-)}$, 20 nm negatively charged RITC-SiNPs; RITC-SiNPs$^{100(+)}$, 100 nm positively charged RITC-SiNPs; RITC-SiNPs$^{100(-)}$, 100 nm negatively charged RITC-SiNPs.

These results could be due to the larger surface area of 20 nm RITC-SiNPs than 100 nm RITC-SiNPs. These results indicated that the RITC-SiNPs could be used for tracing the movement of SiNPs after their oral administration, since they were stable in strong acidic environments without dissociation and release of RITC from the SiNPs.

To monitor the movement of the orally administered RITC-SiNPs, the signal intensities of the whole body images from the IVIS optical imaging system (Figure 5) were assessed and analyzed. After oral administration of the RITC-SiNPs, the majority of the fluorescence signal were visualized from the GI tract. Ex vivo imaging of the isolated major organs from the mice was performed to investigate absorptions and distributions of the RITC-SiNPs after their oral administration (Figure 6). Ex vivo images demonstrated that the RITC-SiNPs were absorbed into the blood from the intestinal tract and were distributed mainly in the lungs, liver, pancreas, and kidneys. In a previous study by Fu et al,[18] administered SiNPs by the oral route were absorbed into the portal vein through the intestine and then transported to the liver, where the distribution process was fast, completing within a few hours. Among the several physical properties of nanoparticles for their influence on absorption and distribution, particle size would be one of the most important factors in determining the kinetics and distribution upon administration into the body.[19–25] For example, Florence et al reported that polystyrene particles with a smaller diameter of 50 and 100 nm could be easily absorbed through Peyer's patches and villi of the GI tract in comparison with larger particles with diameters of 300 and 3,000 nm.[26,27] The distribution of nanoparticles in the liver may be due to the fact that the liver possesses many sinusoidal endothelial cells and Kupffer cells, and it is the major organ for removing circulating foreign materials.[28,29] Furthermore, it was also reported that the distribution of polystyrene particles in the liver were in accordance with particle sizes of 50 nm >200 nm >500 nm >100 nm >25 nm.[30] As shown in Figure 6, the distribution of the 100 nm RITC-SiNPs in the liver was higher than that of the 20 nm RITC-SiNPs. In addition, it was well known that the introduced SiNPs into the circulatory system were eliminated via renal and biliary clearance.[31] For example, Fu et al[18] reported that mesoporous SiNPs with 110 nm of average

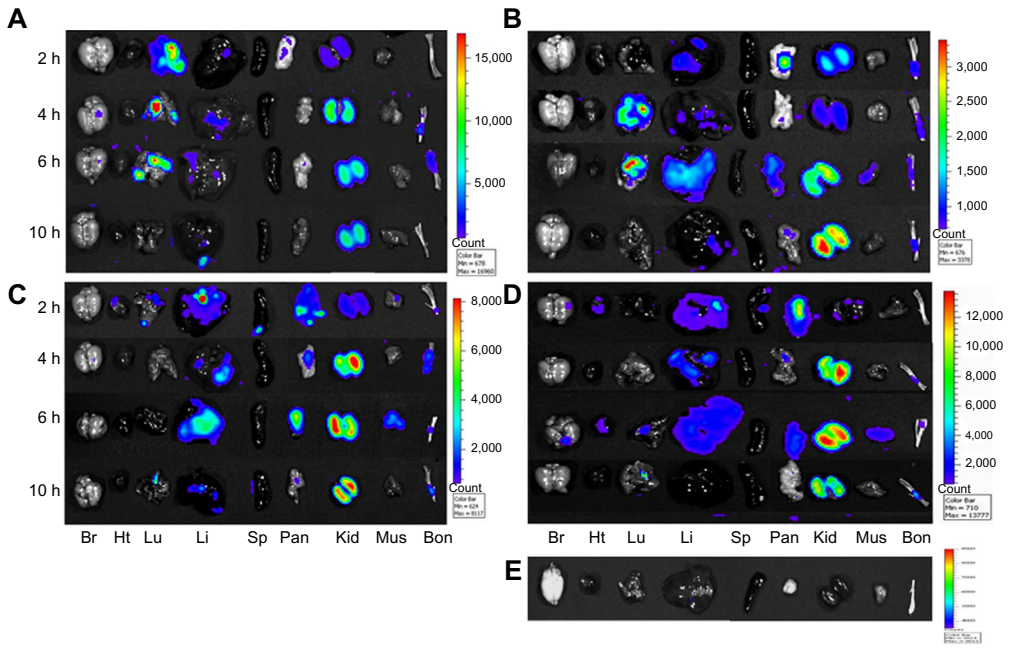

Figure 6 Ex vivo optical images of the major organs in mice that were orally administered with (**A**) RITC-SiNPs$^{20(+)}$, (**B**) RITC-SiNPs$^{20(-)}$, (**C**) RITC-SiNPs$^{100(+)}$, and (**D**) RITC-SiNPs$^{100(-)}$ at 2, 4, 6, and 10 hours post-administration. (**E**) The organs were removed from a healthy mouse without administration of RITC-SiNPs and imaged under the same conditions.

Abbreviations: Bon, bone; Br, brain; Ht, heart; Kid, kidneys; Li, liver; Lu, lungs; Mus, muscle; Pan, pancreas; RITC-SiNP, rhodamine B isothiocyanate-incorporated silica oxide nanoparticle; RITC-SiNPs$^{20(+)}$, 20 nm positively charged RITC-SiNPs; RITC-SiNPs$^{20(-)}$, 20 nm negatively charged RITC-SiNPs; RITC-SiNPs$^{100(+)}$, 100 nm positively charged RITC-SiNPs; RITC-SiNPs$^{100(-)}$, 100 nm negatively charged RITC-SiNPs; Sp, spleen; h, hours.

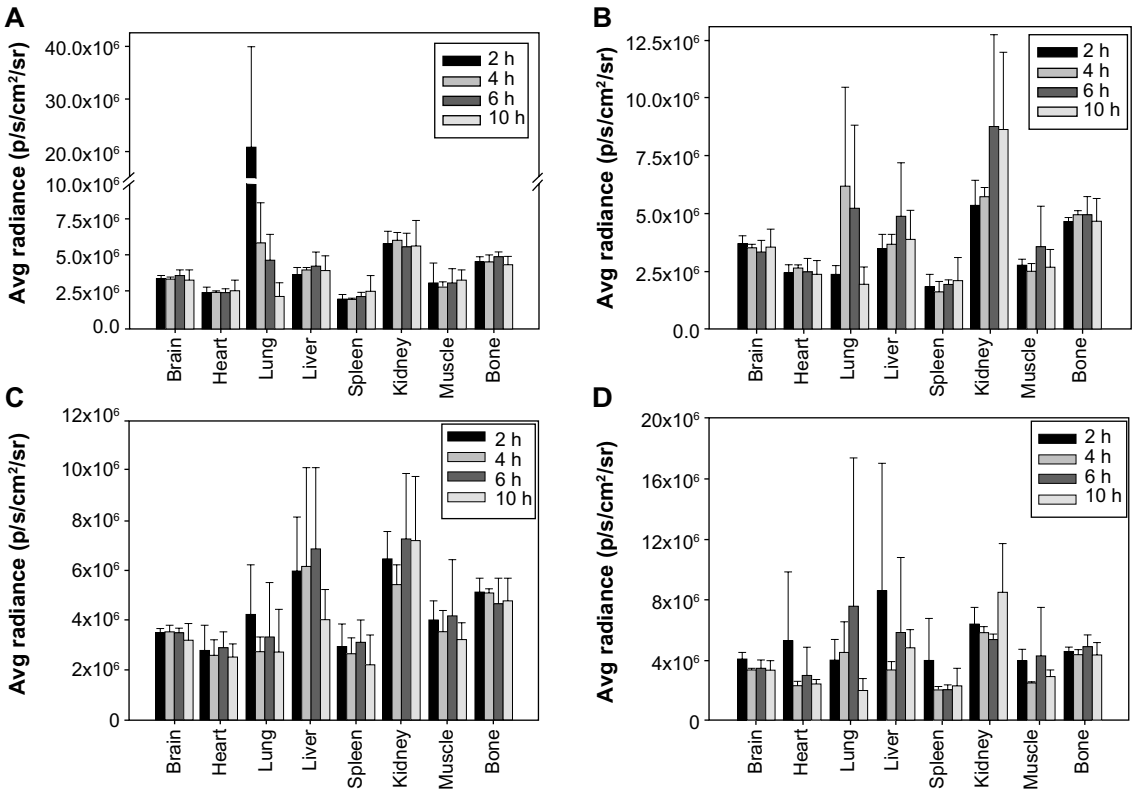

Figure 7 Quantification of ex vivo images: (**A**) RITC-SiNPs$^{20(+)}$, (**B**) RITC-SiNPs$^{20(-)}$, (**C**) RITC-SiNPs$^{100(+)}$, and (**D**) RITC-SiNPs$^{100(-)}$ at 2, 4, 6, and 10 hours post-administration.

Abbreviations: Avg, average; RITC-SiNP, rhodamine B isothiocyanate-incorporated silica oxide nanoparticle; RITC-SiNPs$^{20(+)}$, 20 nm positively charged RITC-SiNPs; RITC-SiNPs$^{20(-)}$, 20 nm negatively charged RITC-SiNPs; RITC-SiNPs$^{100(+)}$, 100 nm positively charged RITC-SiNPs; RITC-SiNPs$^{100(-)}$, 100 nm negatively charged RITC-SiNPs; h, hours.

mean diameter were detected in liver, lung, spleen, and kidney after oral exposure. Furthermore, after oral exposure, the mesoporous SiNPs were observed in urine and were analyzed by TEM. Many previous studies have demonstrated that SiNPs can be excreted through the renal system because they cause damage to the glomerulus and then increase the permeability of the glomerulus.[32] Therefore, the RITC-SiNPs could be translocated into the circulatory system and accumulate in organs, such as liver and lung, and then portions of them would be excreted through the renal system.

Conclusion

In this study, RITC-SiNPs, without chemical conjugation and surface modification, were used to investigate the kinetics of SiNPs. RITC-SiNPs were absorbed into the circulatory system after their oral administration, and afterwards, they were distributed in the lungs, liver, pancreas, and kidneys. The translocations and distribution of RITC-SiNPs after their oral administration were influenced by particle size but not surface charge. The biodistribution and clearances of nanoparticles was monitored by optical imaging. In conclusion, optical imaging studies may provide valuable information to understand the kinetics and toxicity of nanomaterials, including SiNPs.

Acknowledgments

This research was supported by a grant (10182MFDS991) from the Ministry of Food and Drug Safety in 2010. This study was also supported by a grant from the National R&D Program for Cancer Control, Ministry of Health, Welfare and Family Affairs, Republic of Korea (Number 0620220). This work was also supported by Radiation Technology R&D Program through the National Research Foundation of Korea, funded by the Ministry of Education, Science and Technology (2012M2A2A7014020).

Disclosure

The authors report no conflicts of interest in this work.

References

1. Yu Y, Li Y, Wang W, et al. Acute Toxicity of amorphous silica nanoparticles in intravenously exposed ICR mice. *PLoS One*. 2013;8(4):e61346.
2. Yang X, Liu J, He H, et al. SiO_2 nanoparticles induce cytotoxicity and protein expression alteration in HaCaT cells. *Part Fibre Toxicol*. 2010;7:1.
3. Freitas Jr RA. Nanotechnology, nanomedicine and nanosurgery. *Int J Surg*. 2005;3(4):243–246.
4. Li Y, Sun L, Jin M, et al. Size-dependent cytotoxicity of amorphous silica nanoparticles in human hepatoma HepG2 cells. *Toxicol In Vitro*. 2011;25(7):1343–1352.
5. Gong C, Tao G, Yang L, Liu J, He H, Zhuang Z. The role of reactive oxygen species in silicon dioxide nanoparticle-induced cytotoxicity and DNA damage in HaCaT cells. *Mol Biol Rep*. 2012;39(4):4915–4925.
6. Orts-Gil G, Natte K, Österle W. Multi-parametric reference nanomaterials for toxicology: state of the art, future challenges and potential candidates. *RSC Adv*. 2013;3:18202–18215.
7. Lee CM, Jeong HJ, Yun KN, et al. Optical imaging to trace near infrared fluorescent zinc oxide nanoparticles following oral exposure. *Int J Nanomed*. 2012;7:3203–3209.
8. Lee CM, Jeong HJ, Kim DW, Sohn MH, Lim ST. The effect of fluorination of zinc oxide nanoparticles on evaluation of their biodistribution after oral administration. *Nanotechnology*. 2012;23(20):205102.
9. Gibson N, Holzwarth U, Abbas K, et al. Radiolabelling of engineered nanoparticles for in vitro and in vivo tracing applications using cyclotron accelerators. *Arch Toxicol*. 2011;85(7):751–773.
10. Natte K, Behnke T, Orts-Gil G, et al. Synthesis and characterization of highly fluorescent core-shell nanoparticles based on Alexa dyes. *J Nanopart Res*. 2012;14:680.
11. Areses P, Agüeros MT, Quincoces G, et al. Molecular imaging techniques to study the biodistribution of orally administered ^{99m}Tc-labelled naive and ligand-tagged nanoparticles. *Mol Imaging Biol*. 2011;1(6)3:1215–1223.
12. Orts-Gil G, Natte K, Thiermann R, et al. On the role of surface composition and curvature on biointerface formation and colloid stability of nanoparticles in a protein-rich model system. *Colloids Surf B Biointerfaces*. 2013;108:110–119.
13. Chen JK, Shih MH, Peir JJ, et al. The use of radioactive zinc oxide nanoparticles in determination of their tissue concentrations following intravenous administration in mice. *Analyst*. 2010;135(7):1742–1746.
14. He Q, Zhang Z, Gao F, Li Y, Shi J. In vivo biodistribution and urinary excretion of mesoporous silica nanoparticles: effects of particle size and PEGylation. *Small*. 2011;7(2):271–280.
15. Park YH, Bae HC, Jang Y, et al. Effect of the size and surface charge of silica nanoparticles on cutaneous toxicity. *Mol Cell Toxicol*. 2013;9(1):67–74.
16. Kim JS, Yoon TJ, Yu KN, et al. Cellular uptake of magnetic nanoparticle is mediated through energy dependent endocytosis in A549 cells. *J Vet Sci*. 2006;7(4):321–326.
17. Huang X, Li L, Liu T, et al. The shape effect of mesoporous silica nanoparticles on biodistribution, clearance, and biocompatibility in vivo. *ACS Nano*. 2011;5(7):5390–5399.
18. Fu C, Liu T, Liu H, Chen D, Tang F. The absorption, distribution, excretion and toxicity of mesoporous silica nanoparticles in mice following different exposure routes. *Biomaterials*. 2013;34(10):2565–2575.
19. Awaad A, Nakamura M, Ishimura K. Imaging of size-dependent uptake and identification of novel pathways in mouse Peyer's patches using fluorescent organosilica particles. *Nanomed Nanotechnol Biol Med*. 2011;8(5):627–636.
20. Rancan F, Gao Q, Graf C, et al. Skin penetration and cellular uptake of amorphous silica nanoparticles with variable size, surface functionalization, and colloidal stability. *ACS Nano*. 2012;6(8):6829–6842.
21. Moulari B, Pertuit D, Pellequer Y, Lamprecht A. The targeting of surface modified silica nanoparticles to inflamed tissue in experimental colitis. *Biomaterials*. 2008;29(34):4554–4560.
22. Jani PU, McCarthya DE, Florence AT. Nanosphere and microsphere uptake via Peyer's patches: observation of the rate of uptake in the rat after a single oral dose. *Int J Pharm*. 1992;86(2–3):239–246.
23. Jani PU, Halbert GW, Langridge J, Florence AT. Nanoparticle uptake by the rat gastrointestinal mucosa: quantitation and particle size dependency. *J Pharm Pharmacol*. 1990;42(12):821–826.
24. Manisha PD, Vinod L, Gordon LA, Robert JL. Gastrointestinal uptake of biodegradable microparticles: effect of particle size. *Pharm Res*. 1996;13(12):1838–1845.
25. Sass W, Dreyer HP, Seifert J. Rapid insorption of small particles in the gut. *Am J Gastroenterol*. 1990;85(3):255–260.

26. Florence AT. The oral absorption of micro- and nanoparticulates: neither exceptional nor unusual. *Pharm Res*. 1997;14(3):259–266.
27. Florence AT, Hillery AM, Hussain N, Jani PU. Factors affecting the oral uptake and translocation of polystyrene nanoparticles: histological and analytical evidence. *J Drug Target*. 1995;3(1):65–70.
28. Roberts RA, Ganey PE, Ju C, Kamendulis LM, Rusyn I, Klaunig JE. Role of the kupffer cell in mediating hepatic toxicity and carcinogenesis. *Toxicol Sci*. 2007;96(1):2–15.
29. Lanthier N, Molendi-Coste O, Horsmans Y, van Rooijen N, Cani PD, Leclercq IA. Kupffer cell activation is a causal factor for hepatic insulin resistance. *Am J Physiol Gastrointest Liver*. 2010;298(1): G107–G116.
30. Kulkarni SA, Feng SS. Effects of particle size and surface modification on cellular uptake and biodistribution of polymeric nanoparticles for drug delivery. *Pharm Res*. 2013;30(10):2512–2522.
31. Borak B, Biernat P, Preshcha A, Baszczuk A, Pluta J. In vivo study on the biodistribution of silica particles in the bodies of rats. *Adv Clin Exp Med*. 2012;21(1):13–18.
32. Yu T, Greish K, McGill LD, Ray A, Ghandehari H. Influence of geometry, porosity, and surface characteristics of silica nanoparticles on acute toxicity; their vasculature effect and tolerance threshold. *ACS Nano*. 2012;6(3):2289–2301.